Pharm Res (2015) 32:180–195
DOI 10.1007/s11095-014-1454-8

RESEARCH PAPER

Co-Spray Dried Carbohydrate Microparticles: Crystallisation Delay/Inhibition and Improved Aerosolization Characteristics Through the Incorporation of Hydroxypropyl-β-cyclodextrin with Amorphous Raffinose or Trehalose

Maria Inês Amaro • Lidia Tajber • Owen I. Corrigan • Anne Marie Healy

Received: 10 March 2014 / Accepted: 2 July 2014 / Published online: 30 July 2014

ABSTRACT

Purpose To formulate and investigate the physicochemical properties, physical stability and aerosolization characteristics of nanoporous/nanoparticulate microparticles (NPMPs) prepared by co-spray drying the sugars raffinose pentahydrate (R) or trehalose dihydrate (T) with the cyclic oligosaccharide hydroxypropyl-β-cyclodextrin (HPβCD).

Methods Production of powders was carried out using a laboratory scale spray dryer. The resulting powders were characterised by X-ray powder diffraction (XRPD), scanning electron microscopy (SEM), laser diffraction particle sizing, specific surface area analysis (SSA), Fourier transform infrared (FTIR), differential scanning calorimetry (DSC), dynamic vapour sorption (DVS) and aerodynamic assessment using a Next Generation Impactor (NGI).

Results Powders were amorphous and composed of spherical, porous microparticles with reduced particle size and high specific surface area (~100 m^2/g). DSC scans showed a single glass transition temperature. FTIR was indicative of the existence of molecular interactions between the carbohydrates. DVS analysis showed an increase in the critical relative humidity (RH) of raffinose and trehalose and eventual crystallization inhibition with increasing concentration of HPβCD. The *in vitro* deposition showed powders formulated with HPβCD had higher recovered emitted dose and fine particle fraction (<5 μm) than raffinose and trehalose spray dried alone.

Conclusions The co-spray drying of raffinose or trehalose with HPβCD results in powders with improved physicochemical characteristics, physical stability and aerodynamic behaviour compared to spray-dried raffinose/trehalose particles, constituting improved potential drug-carrier systems for pulmonary delivery.

KEY WORDS areosolization · crystallisation · hydroxypropyl-β-cyclodextrin · raffinose · stability · trehalose

INTRODUCTION

Non-reducing sugars, such as raffinose and trehalose, possess properties that make them promising excipients for protection of biomolecules. They appear to be effective stabilisers of proteins in the amorphous state [1–3]. Studies by Lopéz-Diéz *et al.* [4], Maury *et al.* [3], Yoshii *et al.* [5] and Ní Ógáin *et al.* [6] have established the protective action of trehalose and raffinose on protein integrity, reducing loss of bioactivity. Carpenter and Crowe [7, 8] suggested the water replacement theory to explain the protective action of the sugar compounds. In this theory, when water is removed H-bonds are formed between the excipient and the biomolecule, maintaining the structural integrity of the peptide or protein. A second theory of protein protection through the use of such sugars was proposed by Franks *et al.* [9] based on the formation of an amorphous glass during drying, which provides a rigid matrix around the protein molecules to restrict and stabilise their motion.

Ní Ógáin *et al.* [6] reported on nanoporous/nanoparticulate microparticles (NPMPs) of raffinose or trehalose and demonstrated that the porous morphology of such microparticles was retained on the incorporation of a model protein into the particles. The protein-containing sugar-based microparticles were demonstrated to have suitable micromeritic and aerosolization characteristics for pulmonary delivery.

The effect of operating parameters of a laboratory spray dryer on powder characteristics was subsequently reported,

Electronic supplementary material The online version of this article (doi:10.1007/s11095-014-1454-8) contains supplementary material, which is available to authorized users.

M. I. Amaro • L. Tajber • O. I. Corrigan • A. M. Healy (✉)
School of Pharmacy and Pharmaceutical Sciences, Trinity College
University of Dublin, Dublin 2, Ireland
e-mail: healyam@tcd.ie

with a view to optimising the production of raffinose and trehalose NPMPs, intended to be used as carriers of biomolecules for inhalation, maximising the application of the protective nature of these non-reducing sugars [10]. However, raffinose and trehalose present the risk of recrystallisation and loss of bioprotective effectiveness due to their amorphous nature after spray drying. Materials in this solid-state are known to be less stable physically and chemically than their crystalline counterparts [11–13]. Amorphous sugar powders such as glucose, lactose, raffinose, trehalose and sucrose will spontaneously sorb (adsorb or absorb) a significant amount of water vapour from their surroundings unless stored under completely dry conditions; this sorbed water vapour can markedly change the physical and chemical properties of the sugars, accelerating hydrolytic degradation, isomerisation, and/or crystallisation processes and thus can have a significant impact upon their use and function in pharmaceutical dosage forms such as peptide and protein formulations [11]. Different studies have determined a rapid water absorption and recrystallisation of amorphous raffinose and trehalose powders when exposed to ~75% relative humidity (RH) for 24 h [14–16]. Ní Ógáin *et al.* [6] reported that exposure of trehalose or raffinose:lysozyme NPMP composite systems to 60% RH for 24 h resulted in particle morphology changes and amorphous state conversion into the crystalline state.

Studies by Davidson and Sun [17, 18], Buera *et al.* [19] and Leinen and Labuza [20] have used carbohydrate mixtures of raffinose or trehalose and sucrose to delay and inhibit amorphous sucrose recrystallisation. These studies concluded that an increased ratio of raffinose or trehalose in the system increased the glass transition temperature and decreased the melting enthalpy, enhancing sucrose stability.

Drug stability improvement is nowadays often achieved by means of solid dispersions, which incorporate a higher molecular weight compound, such as an oligosaccharide or a polymer and a drug, to enhance stability and prevent crystallisation of the drug by increasing the glass transition temperature (T_g), through molecular interactions between the drug and polymer and by the antiplasticisation effect (or water scavenger activity) of the polymer [21]. Mazzobre *et al.* [22] applied the solid dispersion approach to an excipient by studying the effect of delaying crystallisation of trehalose in trehalose:lactase systems by the addition of maltodextrin in a ratio of 80:20 (maltodextrin:trehalose). Results showed an increase in the T_g of the system and a delay in trehalose recrystallisation, with improvement of lactase stability at high relative humidity.

Hydroxypropyl-β-cyclodextrin (HPβCD) is a cyclodextrin (CD) produced by replacement of βCD hydroxyl groups by hydroxypropyl ones, resulting in an amorphous form with a molecular weight of 1,541.24 g/mol [23–25]. Its known uses include: improvement of drug solubility and bioavailability by increasing drug molecule permeability; enhancement of drug stability by complex formation or by increasing the system thermal stability (increasing glass transition temperature) [23, 25, 26].

Branchu *et al.* [27] tested the use of sucrose and HPβCD as stabilizing excipients in the spray-drying of a model protein, β-galactosidase. Spray-drying significantly inactivated the enzyme; when processed in the presence of sucrose inactivation still occurred. However, after spray drying β-galactosidase in the presence of HPβCD, or HPβCD and sucrose, full catalytic activity was exhibited on reconstitution, that is, no inactivation occurred upon processing. Furthermore, the reconstituted product was unchanged in terms of molecular weight, charge, and thermal stability, indicating that HPβCD is a potential stabilising excipient.

Based on the aforementioned studies it was intended to spray-dry composite systems of raffinose: HPβCD (R:HPβCD) and trehalose:HPβCD (T:HPβCD), in order to improve trehalose and raffinose NPMP stability, enhancing the biomolecule carrier system previously developed for oral inhalation. The cyclodextrin is added to the formulation to increase the water scavenger capacity of the system and to improve the thermal stability by increasing the glass transition temperature of the composite amorphous systems, with the combined intentional effect of improving physical stability. In addition the effect of the new formulation on powder aerosolization was also studied.

MATERIALS AND METHODS

Materials

d-Raffinose pentahydrate, d-(+)-trehalose dihydrate and potassium bromide (KBr) were purchased from Sigma-Aldrich (Ireland). Hydroxypropyl-β-cyclodextrin was purchased from Janssen Biotech N.V. (Belgium). Solvents used were: n-butyl acetate purchased from Merck (UK), methanol and ethanol were obtained from Lab Scan Analytical Sciences (Ireland) and, deionised water was obtained from a Purite Prestige Analyst HP (Purite Limited, UK) water purification system. Coumarin-6 was purchased from Polysciences Inc., U.S.A..

Preparation of Carbohydrate Composite Systems

Raffinose:HPβCD and trehalose:HPβCD were spray dried as solutions presenting a total solute concentration of 2.9% (*w/v*) and 1% (*w/v*) respectively, using a Büchi Mini Spray dryer B-290 operating in the closed mode with an inert loop B-295 accessory (Büchi, Switzerland). A 0.7 mm nozzle tip and a 1.5 mm diameter nozzle screw cap were used. Solutions were

composed of methanol:n-butyl acetate mixture in a 4:1 (*v*/*v*) proportion. Sugar:cyclodextrin weight ratios varied from 80:20 to 20:80. Nitrogen (at 6 bar) was used as the drying gas in a co-current mode. Spray drying parameters were set as for optimised raffinose and trehalose NPMP production, as previously described by Amaro *et al.* [10]. Spray dried particles were separated from the drying gas using a high-performance cyclone (Büchi, Switzerland). For *in vitro* aerosol deposition studies of the spray dried powders, a fluorescent marker (coumarin-6) was incorporated at a low loading (0.2% by weight of solid content) during spray-drying, to enable subsequent quantitation of powder [6, 28, 29]. Ní Ógáin *et al.* [6] have previously shown the inclusion of this marker to have no impact on the morphology of spray dried raffinose and trehalose porous particles.

X-ray Powder Diffraction (XRPD)

The solid-state nature of powders was determined by X-ray powder diffraction measurements using a Rigaku MiniFlex II desktop X-ray diffractometer (Rigaku, Japan) with Haskris (USA) WA1 cooling unit. The Rigaku MiniFlex II diffractometer consists of a vertical goniometer with a 1.25° dispersion slit, a 1.25° antiscatter slit and a 0.3 mm receiving slit. The Cu anode X-ray tube was operated at 30 kV and 15 mA in combination with a Ni filter to give monochromatic Cu Kα X-rays. Measurements were taken from 5 to 40° on the two θ scale at a step size of 0.05 °/s [6].

Scanning Electron Microscopy (SEM)

SEM micrographs of spray-dried materials were made by means of a MiraTescan XMU (Czech Republic). The samples were fixed on aluminum stubs using double-sided adhesive tape and sputter-coated with gold. Visualisation was performed at 5 kV and photo micrographs were taken at different magnifications in more than one region of the sample, as reported by Amaro *et al.* [10].

Particle Size (PS)

The particle size distributions of the spray-dried powders were determined using a Mastersizer 2000 laser diffraction instrument (Malvern Instruments, UK) with a dry powder sample dispersion accessory (Scirocco 2000). Pressure was set at 2 bar and a vibration feed rate of 50% was used in order to achieve an obscuration between 0.5 and 6% [6, 10]. Samples were run in triplicate. Mastersizer 2000 software was used for data evaluation. The d_{50} reported is the geometric median particle size; the d_{10} and d_{90} are the particle diameters at 10 and 90% of the cumulative volume distribution, respectively. The span of the volume distribution, a measure of the width of the distribution relative to the median diameter, was calculated according to the following equation [30]:

$$span = \frac{\left[d_{(90)} - d_{(10)}\right]}{d_{(50)}} \quad (1)$$

Specific Surface Area (SSA)

SSA of spray-dried powders was measured by gas adsorption using a Micromeritics Gemini VI surface area and pore size analyzer (Micromeritics, U.K.). Adsorption measurements were performed with nitrogen gas as the analytical (adsorptive) gas and helium as the reference gas for free space measurements. Prior to analysis the samples were degassed under nitrogen gas, using a Micromeritics SmartPrep degasser for 24 h at 25°C to remove residual solvent content [6, 10]. The evacuation conditions used in the analysis were as follows: rate of 500 mmHg/min, time 1 min. Equilibration time for adsorption was 10 s. The amounts of nitrogen gas adsorbed at a range of relative pressures (six), $0.05 < P/P_0 < 0.30$, were determined in order to calculate SSA by the Brunauer, Emmett and Teller (BET) method. Analysis was performed in triplicate for each sample.

Bulk and Tapped Density

Bulk and tapped density measurements were performed as previously described [6, 31]. Bulk density (bρ) was calculated by determining the weight of powder required to occupy a 1 ml volume in a graduated glass syringe (Lennox Laboratory supplies, Dublin, Ireland), by pouring under gravity. The tapped density (tρ) of the powders was determined by vertically tapping this sample onto a level bench-top surface from a height of 5 cm 100 times. The tapped density was calculated as the ratio of the mass to the tapped volume of the sample. Each measurement was performed in triplicate.

Solid-State Fourier Transform Infrared Spectroscopy (FTIR)

Infrared spectra of samples were evaluated in order to detect possible molecular modifications after processing of excipients. Spectra were recorded on a Nicolet Magna IR 560 E.S.P. (USA) spectrophotometer equipped with MCT/A detector, working under Omnic software version 4.1. A spectral range of 650–4,000 cm^{-1}, resolution 2 cm^{-1}, and accumulation of 64 scans were used in order to obtain good quality spectra [6]. A KBr disk was used. Samples were mixed with KBr at a ratio of 1:100 using an agate mortar and pestle. Disks were compressed at 8 tones pressure for 1 to 2 min using a 13 mm KBr die set (Apollo Scientific, U.K.). The raw absorption spectra were baseline corrected and smoothed. Each measurement was performed at least in duplicate.

Differential Scanning Calorimetry (DSC)

DSC scans were taken for all the raw materials and spray dried powders by means of a power compensated Mettler Toledo DSC 821e (Switzerland) differential scanning calorimeter with a LabPlant RP-100 refrigerated cooling system. Nitrogen was used as the purge gas. Samples were loaded into 40 μL sealed aluminium pans with three vent holes and scanned over a temperature range of 25–200/300°C with a scanning rate of 10°C/min [6]. Weights of approximately 4 mg were tested. The DSC system was controlled by Mettler Toledo STARe software (version 6.10). The glass transition temperature was defined as the midpoint of the transition and the recrystallisation and melting points are reported as the onsets of the exo/endothermic processes. Each measurement was performed in triplicate.

Dynamic Vapour Sorption (DVS)

Vapour sorption of spray-dried powders was investigated by means of an automated gravimetric vapour sorption analyser, DVS Advantage-1 (Surface Measurements Systems Ltd, UK). The DVS Advantage-1 uses a Cahn D200 recording ultramicrobalance with a mass resolution of ±0.1 μg; the vapour partial pressure around the sample is controlled by mixing saturated and dry carrier gas streams (N_2) using electronic mass flow controllers [32]. Samples were equilibrated at 0% RH until dry and the reference mass was recorded. The samples were exposed to the following relative humidity (% RH) profile: 0 to 90% in 10% steps and the reverse for desorption at 25.0±0.1°C. At each stage, the sample mass was allowed to reach equilibrium, defined as dm/dt=0.002 mg/min over 10 min, before the RH was changed. The amount of water uptake for each RH stage was expressed as a % of the dry sample mass (m_0).

For data analysis the Young-Nelson model was fitted to the vapour sorption isotherm, using the software provided by SMS Ltd. and as previously described by Bravo-Osuna *et al.* [33] and Tewes *et al.* [34]. The following equations were used:

$$M_s = A(\beta + \theta) + B\theta RH \tag{2}$$

$$M_d = A(\beta + \theta) + B\theta RH_{max} \tag{3}$$

where M_s and M_d are, respectively, the mass percentage of water contents of the polymer system at the equilibrium for each %RH, during sorption and desorption. A and B are constants characteristic of each material: $A = \frac{\rho_w Vol_M}{W_m}$ and $B = \frac{\rho_w Vol_A}{W_m}$ where ρ_w is the water density, Vol_M and Vol_A are, respectively, the adsorbed and absorbed water volumes and Wm is the weight of dry material. In this model, θ is the fraction of the material surface covered by at least one layer of water molecules. It is defined as follows, with E a constant depending on the material.

$$\theta = \frac{RH}{(RH + E(1-RH))} \tag{4}$$

And β is defined by the following equation:

$$\beta = \frac{-E \times RH}{(E-RH \times (E-1))} + \frac{E^2}{(E-1)} \times \ln\left[\frac{E-RH(E-1)}{E}\right] - (E+1) \times \ln(1-RH) \tag{5}$$

Thus, Aθ is the mass of water in a complete adsorbed monolayer expressed, like all masses in the model, as a fraction of the dry mass of the solid. A(β+θ) is the total amount of adsorbed water, and Aβ is the mass of water which is adsorbed beyond the mass of the monolayer, that is, in multilayers. B is the mass of absorbed water at 100% RH, and, hence, BθRH is the mass of absorbed water when the monolayer coverage is θ for a given %RH. According to the model characteristics, from the estimated values of A, B, and E, the corresponding profiles of water adsorbed in monolayer (Aθ), multilayer (Aβ) and absorbed water (BθRH) were obtained.

In Vitro Aerosol Deposition Studies Using the Next Generation Impactor (NGI)

The *in vitro* deposition of the dry powders was evaluated using a NGI (Copley Scientific Limited, Nottingham, UK) operated under pharmacopoeial conditions [35]. The flow rate was adjusted to achieve a pressure drop of 4 kPa in the powder inhaler (Handihaler®, Boehringher Ingelheim, Ingelheim, Germany) and the time of aspiration was adjusted to obtain 4 L air flow [10, 34]. The air flow rate and effective cut-off diameter are provided in the supplementary material associated with this article as Table 1S. The dry powder inhaler was loaded with a no. 3 hard gelatin capsule loaded with 20±2 mg of powder for each test. After dissolution in a appropriate volume of ethanol 80% (*v*/*v*):water 20% (*v*/*v*), particle deposition in the device, the throat and the stages and the filter was determined by fluorescence detection, as previously described by Ní Ógáin *et al.* [6]. Each test was repeated three times. The total amount of particles with aerodynamic diameters smaller than 5.0 μm was calculated by interpolation from the inverse of the standard normal cumulative mass distribution less than stated size cut-off against the natural logarithm of the cut-off diameter of the respective stages. This amount was considered as the fine particle fraction (FPF) (or respirable fraction) and expressed as a percentage of the emitted recovered dose (ED). The mass median aerodynamic diameter (MMAD) of the particles was determined from the same plot

as the particle size corresponding to the 50% point of the cumulative distribution, and the geometric standard deviation (GSD):

$$GSD = \sqrt{\frac{sizeX}{sizeY}} \quad (6)$$

Where X is the particle size corresponding to the 84% point and size Y is the particle size corresponding 16% point of the cumulative distribution [28].

Statistical Data Analysis

Statistical analysis of variance, ANOVA followed by the posthoc Tukey's test, was performed when there were more than two sets of data, to determine the significance (p-value) of an effect or difference between means, using Minitab™ software (version 13.32). Parameters found to be significant at at least the 95% confidence level were considered to have an effect or to be different.

Descriptive statistics (median and standard deviation) were determined using Microsoft® Office Excel®.

RESULTS

All spray-dried composites were amorphous as shown by XRPD analysis (Figs. 1 and 2). Diffractograms presented the typical diffuse halo pattern, characteristic of amorphous materials. The halo pattern changed with increasing HPβCD concentration in the system. Amorphous halo shape may be related to short-range order within the amorphous material. HPβCD presents two broad peaks probably due to its molecular arrangement as a cup that can form small domains with some degree of short-range order [25, 36]. In trehalose composites system, the two broad peaks were more evident than in

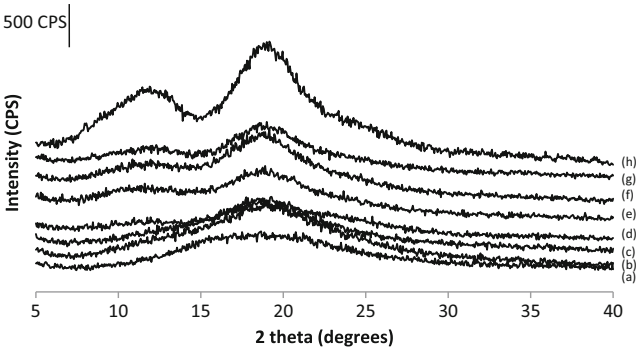

Fig. 1 XRPD of spray dried R:HPβCD composite systems at ratios: (**a**) 100:0, (**b**) 80:20, (**c**) 70:30, (**d**) 60:40, (**e**) 40:60, (**f**) 30:70, (**g**) 20:80 and (**h**) 0:100.

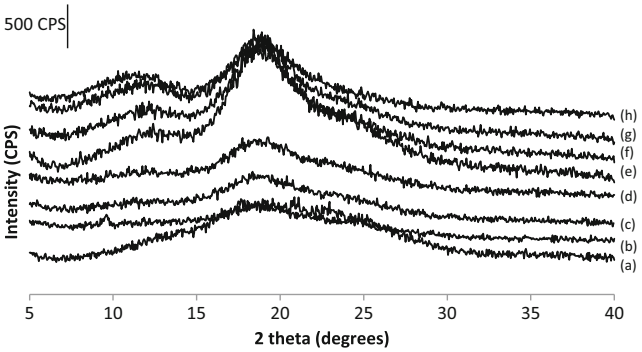

Fig. 2 XRPD diffractograms of spray dried T:HPβCD composite systems at ratios: (**a**) 100:0, (**b**) 80:20 (**c**) 70:30, (**d**) 60:40, (**e**) 40:60, (**f**) 30:70, (**g**) 20:80 and (**h**) 0:100.

the raffinose composite systems, which can be hypothesized to be a result of different molecular packing, due the non-reducing sugars presenting different molecular orientations. Spray-drying of R:HPβCD and T:HPβCD composite systems led to the conversion of the crystalline sugars into a disordered amorphous state. The addition of the second excipient (i.e. HPβCD) to raffinose and trehalose NPMPs did not affect the particle morphology, maintaining the characteristic nanoporous/nanoparticulate morphology described by Ní Ógáin *et al.* [6] and Amaro *et al.* [10]. SE micrograph examples for each type of composite can be found in Fig. 3.

Particle size volume distributions for all composite systems were narrow and monomodal with low span values (between 1.1 and 1.2 for R:HPβCD and between 1.0 and 1.2 for T:HPβCD). The geometric median particle size (d_{50}) for R:HPβCD particles was in the range of 1.7–2.0 μm and for T:HPβCD particles was in the range 1.5–1.6 μm. Tables I and II present the reported values of d_{10}, d_{50}, d_{90} and percentage of particles with size <1 μm as mean ± standard deviation. ANOVA of the particle size distributions pointed out statistically significant differences between d_{50}, d_{90} and the percentage of particles with diameter below 1 μm ($p<0.05$) for R:HPβCD spray-dried systems: the d_{50} and d_{90} of R:HPβCD were different from raffinose spray dried alone ($p=0.000$ for d_{50} and d_{90}); the system comprising 40% cyclodextrin showed a significant increase in submicron-size particles ($p=0.021$), distinguishing it from the other R:HPβCD samples. The addition of cyclodextrin to trehalose did not significantly affect the particle size distribution, at a confidence level of 95%.

Specific surface area was also investigated as a reflection of porosity associated with porous particles such as the NPMPs [31]. A trend was seen with both types of composite systems - the addition of the cyclodextrin to raffinose or trehalose NPMPs increased the surface area, hence increasing the porosity (Tables I and II). This increase was not linear with the increase of weight fraction of HPβCD; a maximum SSA value

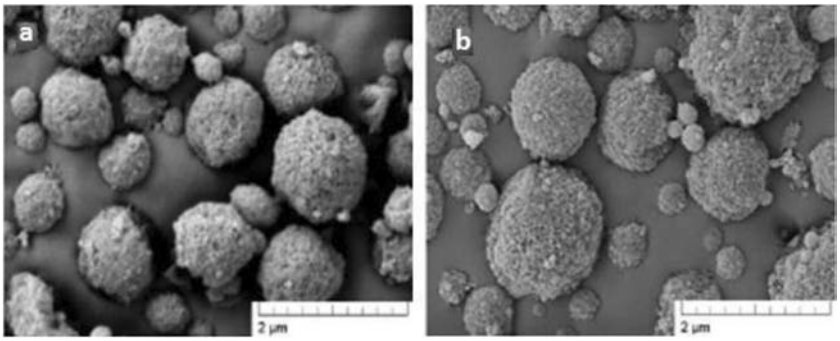

Fig. 3 SE micrographs examples of (**a**) R:HPβCD composite systems (**b**) T:HPβCD composite systems.

of 106.96±0.07 m^2/g for R:HPβCD and 102.79±0.17 m^2/g for T:HPβCD was achieved at 40% weight of cyclodextrin, after which SSA decreased to values closer to the surface area of HPβCD when spray dried alone. ANOVA showed spray-dried systems to be significantly different from raffinose or trehalose spray-dried alone ($p<0.05$).

Bulk and tap density results for R:HPβCD and T:HPβCD are represented in Tables I and II. All samples presented values below 0.3 g/cm^3 making them suitable for pulmonary delivery according to Bosquillon *et al.* [37].

Infrared absorption measurements were carried out to evaluate possible interactions between the materials. Figures 4 and 5 show the IR spectra for raffinose pentahydrate, trehalose dihydrate, HPβCD as supplied and all spray dried carbohydrate composite systems; the crystalline materials presented sharp absorption bands, whereas HPβCD as supplied and the spray dried composite systems showed much broader absorption bands, typical of amorphous materials. IR spectra of crystalline and amorphous states of both raffinose and trehalose have been well characterized in studies by Wolkers *et al.* [38], Akao *et al.* [39], Wolkers *et al.* [40] and Cheng and Lin [41]. The cyclodextrin (HPβCD) IR spectra has been reported by Williams III, *et al.* (1998), Misiuk and Zalewska [42] and Wu *et al.* [43]. In general, bands detected in the spray dried composites were consistent with those reported for individual sugar and cyclodextrin materials.

The nature of the molecules used in this study suggests a potential for H-bonding between them. Thus, it is thought that the broad feature of the band between 3,600 and 3,000 cm^{-1}, detected in all spray-dried systems spectra, is attributed to O-H stretching vibrations (inherent to the molecules itself) and to the establishment of hydrogen bonds among raffinose or trehalose and HPβCD molecules. In addition, bands in the region between 1,200 and 900 cm^{-1}, seemed to transit from raffinose or trehalose fingerprint to the cyclodextrin fingerprint as the concentration of the latter was increased; possibly due to an overlapping of bands [42]. Such overlapping also resulted in the suppression of the raffinose and trehalose α-(1→6)/α-(1→1) glycosidic bond band at 980/948 and 979/937 cm^{-1} respectively.

DSC scans of spray dried composite systems showed a single glass transition that was an intermediate between the glass transition temperature (T_g) values of the spray-dried materials alone (Tables I and II, Figs. 6 and 7); a significant

Table I Particle Size (*PS*), Specific Surface Area (*SSA*), Bulk (*bp*) and Tap (*tp*) Density, and Glass Transition Temperature (T_g) of R:HPβCD Composite Systems. ANOVA is also Presented for Significance ($p<0.05$) of Differences Between Means ($n=3$, Mean ± Standard Deviation)

	100:0	80:20	70:30	60:40	40:60	30:70	20:80	0:100
PS (µm)								
d_{10}**	1.1±0.02	1.1±0.01	1.1±0.00	1.1±0.00	1.1±0.04	1.1±0.00	1.1±0.00	1.1±0.00
d_{50}*	1.7±0.01	1.9±0.01	1.9±0.01	1.9±0.00	1.9±0.01	1.9±0.00	1.9±0.01	2.0±0.00
d_{90}*	2.9±0.04	3.4±0.02	3.2±0.01	3.3±0.01	3.3±0.16	3.2±0.01	3.5±0.03	3.5±0.14
<1 µm (%)***	7.2±0.71	7.0±0.23	5.7±0.25	8.4±0.01	7.0±1.48	5.8±0.07	6.6±0.12	6.6±0.12
SSA (m^2/g)*	58.16±0.51	75.84±0.12	91.32±0.27	106.96±0.07	91.52±0.01	95.48±0.08	94.21±0.12	81.08±0.03
bp (g/cm^3)*	0.15±0.01	0.14±0.01	0.15±0.01	0.13±0.00	0.13±0.01	0.14±0.00	0.10±0.00	0.16±0.00
tp (g/cm^3)*	0.24±0.00	0.24±0.03	0.26±0.02	0.22±0.01	0.22±0.01	0.26±0.01	0.19±0.00	0.29±0.00
T_g (°C)*	115.6±0.21	115.0±0.35	117.1±0.11	117.5±0.27	120.8±0.26	165.6±0.85	192.9±0.88	225.4±0.32

* $p=0.000$

** $p=0.056$

*** $p=0.021$

Table II Particle Size (*PS*), Specific Surface Area (*SSA*), Bulk (*bp*) and Tap (*tp*) Density, and Glass Transition Temperature (T_g) of T:HPβCD Composite Systems. ANOVA is also Presented for Significance ($p < 0.05$) of Differences Between Means ($n = 3$, Mean ± Standard Deviation)

	100:0	80:20	70:30	60:40	40:60	30:70	20:80	0:100
PS (μm)								
d_{10} **	0.9 ± 0.02	0.8 ± 0.13	1.0 ± 0.00	0.9 ± 0.05	0.9 ± 0.00	0.9 ± 0.01	0.9 ± 0.01	0.9 ± 0.01
d_{50} ***	1.6 ± 0.02	1.6 ± 0.04	1.6 ± 0.01	1.5 ± 0.01	1.5 ± 0.00	1.6 ± 0.02	1.6 ± 0.02	1.5 ± 0.01
d_{90} *	2.7 ± 0.03	2.2 ± 0.11	2.6 ± 0.01	2.6 ± 0.01	2.7 ± 0.00	2.8 ± 0.01	2.7 ± 0.04	0.9 ± 0.01
< 1 μm (%)****	13.0 ± 10.1	11.2 ± 2.04	12.5 ± 0.20	15.2 ± 0.49	15.4 ± 0.18	15.1 ± 1.90	15.6 ± 0.74	16.8 ± 0.45
SSA (m^2/g)*	51.44 ± 0.49	86.24 ± 0.22	91.06 ± 0.14	102.79 ± 0.17	102.20 ± 0.01	89.39 ± 0.10	84.92 ± 0.02	82.82 ± 0.04
bp (g/cm^3)*	0.15 ± 0.01	0.15 ± 0.002	0.10 ± 0.001	0.14 ± 0.003	0.12 ± 0.004	0.11 ± 0.004	0.14 ± 0.003	0.17 ± 0.003
tp (g/cm^3)*	0.22 ± 0.01	0.25 ± 0.01	0.20 ± 0.01	0.26 ± 0.02	0.24 ± 0.01	0.24 ± 0.02	0.27 ± 0.01	0.31 ± 0.01
T_g (°C)*	121.8 ± 0.45	120.3 ± 1.75	119.3 ± 0.40	120.6 ± 0.76	153.7 ± 1.03	166.5 ± 1.04	193.4 ± 0.37	225.4 ± 0.32

* $p = 0.000$
** $p = 0.106$
*** $p = 0.167$
**** $p = 0.001$

increase in T_g ($p < 0.05$) was observed with increasing content of cyclodextrin. No evidence of further thermal events such as crystallisation or melting was found for R:HPβCD systems for the temperature range investigated. On the other hand, T:HPβCD systems presented delayed and reduced enthalpy of crystallisation and melting events with increasing content of cyclodextrin, compared to trehalose spray dried alone, with total inhibition of both events when the cyclodextrin weight fraction was ≥60%, suggesting an enhancement of trehalose physical stability when mixed with HPβCD. Studies on HPβCD have shown that this oligosaccharide is able to decrease the degree of crystallinity and inhibit recrystallisation of polymers and drugs, reducing the melting enthalpy and increasing their physical stability [25, 34, 44].

For a thorough analysis of the composite systems glass transition temperatures and in order to gain more knowledge on the physical properties of the systems, different model equations of T_g prediction were used and fitted to the experimental data:

– Gordon-Taylor (GT) equation with Simha-Boyer rule:

$$T_g = \frac{w_1 T_{g1} + K_{GT} w_2 T_{g2}}{w_1 + K_{GT} w_2} \quad (7)$$

where $K_{GT} = \frac{d_1 T_{g1}}{d_2 T_{g2}}$, assuming ideal volume additivity of both materials at T_g, no specific interactions between the two components and the effect of density is accounted for; T_g, w and d are the glass transition temperature in degrees Kelvin, the weight fraction and density of the subscripts *1* (first component), *2* (second component) and mixture (no subscript), K_{GT} is related to a thermal expansion coefficient difference between glassy and liquid [35, 45–47];

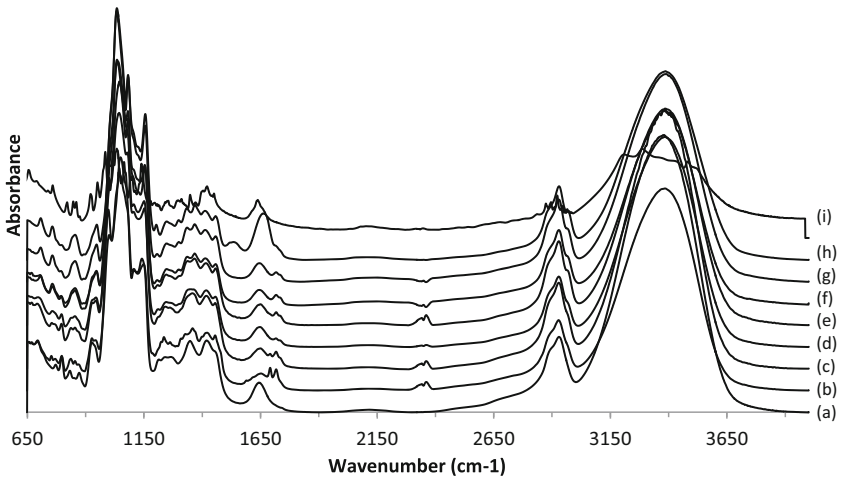

Fig. 4 FTIR spectra of spray dried R:HPβCD composite systems at ratios (**a**) 100:0, (**b**) 80:20, (**c**) 70:30, (**d**) 60:40, (**e**) 40:60, (**f**) 30:70, (**g**) 20:80 (**h**) 0:100 and (**i**) raffinose pentahydrate.

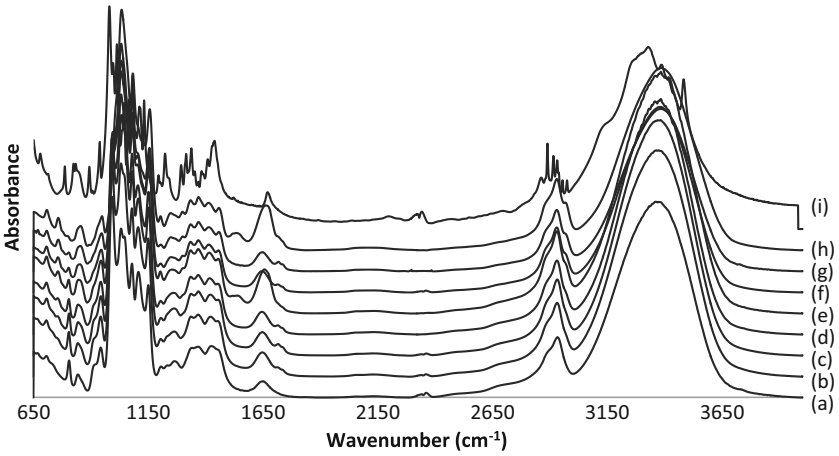

Fig. 5 FTIR spectra of spray dried T:HPβCD composite systems at ratios (**a**) 100:0, (**b**) 80:20, (**c**) 70:30, (**d**) 60:40, (**e**) 40:60, (**f**) 30:70, (**g**) 20:80, (**h**) 0:100 and (**i**) trehalose dihydrate.

– Fox equation assuming components have similar density [45–47]:

$$\frac{1}{T_g} = \frac{w_1}{T_{g1}} + \frac{w_2}{T_{g2}} \tag{8}$$

– Kwei equation is an extension of the GT equation, used in cases of strong interactions between components:

$$T_g = \frac{w_1 T_{g1} + K_k w_2 T_{g2}}{w_1 + K_k w_2} + q w_1 w_2 \tag{9}$$

where K_k and q are fitted values to experimental data [45, 47].

Figure 8 and Table III present the obtained results from the model equations fitted to raffinose and trehalose composite systems. All systems demonstrated deviations to predictions by the Gordon-Taylor and Fox equations. For R:HPβCD systems only one experimental point was fitted by the Gordon-Taylor and Fox equations, with the remaining points falling below the predicted curve (negative deviations). In the case of T:HPβCD systems all glass transitions presented a negative deviation from the calculated T_g. Given the observed deviations, there was the need to find a more suitable model for T_g prediction – the Kwei equation (Eq. 9). The Kwei equation presented a good fit to R:HPβCD (R^2=0.902) and a very good fit for T:HPβCD data (R^2=0.983), hence interactions between molecules, such as hydrogen bonding and other intermolecular interactions, could be hypothesised. Some data points presented very small deviations from predicted values; these might be due to plasticising effects of the residual solvent content in powders after spray drying [45]. The constant q in Eq. 9 (qw_1w_2) is proportional to the number of specific interactions existing in the mixture, with q as a measure of the efficacy of hydrogen bond formation; hence a larger magnitude of q, without regard to its sign, is indicative of a higher degree of hydrogen bonds between the mixture components, with q=0 indicating no H-bonding between molecules [48]. Table III reports the q value for the spray-dried systems. The calculated q value for raffinose composite systems was −165.66 and for T:HPβCD composite systems was −140.15, suggesting a high interaction between molecules due to hydrogen bonding.

DVS was used to evaluate the effect of moisture on the solid-state stability of the different composite systems in comparison to the materials spray dried alone. It was expected that the inclusion of HPβCD would lead to an increase in the water scavenger/uptake capacity of the spray dried systems, relative

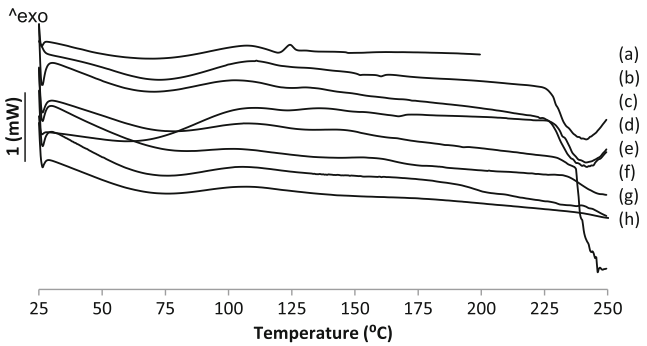

Fig. 6 DSC scans of R:HPβCD composite systems at ratios: (**a**) 100:0, (**b**) 80:20, (**c**) 70:30, (**d**) 60:40, (**e**) 40:60, (**f**) 30:70, (**g**) 20:80 and (**h**) 0:100.

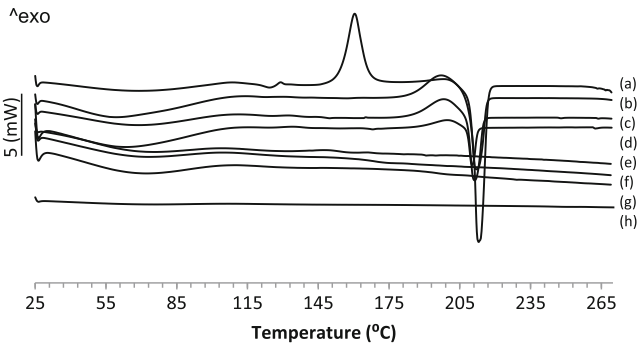

Fig. 7 DSC scans of T:HPβCD composite systems at ratios (**a**) 100:0, (**b**) 80:20, (**c**) 70:30, (**d**) 60:40, (**e**) 40:60, (**f**) 30:70, (**g**) 20:80 and (**h**) 0:100.

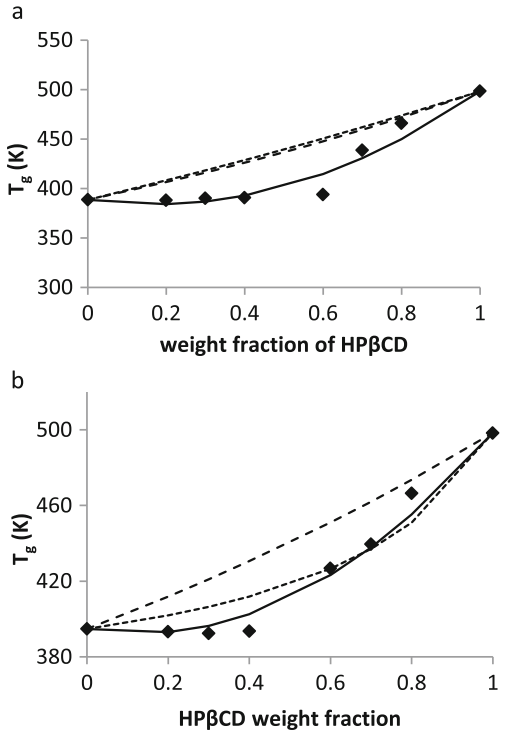

Fig. 8 Glass transitions (T_g) of (**a**) R:HPβCD, (**b**) T:HPβCD composite systems as a function of the added excipient weight fraction. The dotted, dashed and solid lines represent the predictions based on the Gordon-Taylor and Fox and Kwei equations, respectively.

to systems comprised of raffinose or trehalose alone. Figure 9 shows the water vapour sorption isotherms for the materials spray dried alone.

Spray dried trehalose takes up approximately 11% by mass of moisture below 50% RH, presenting, above this RH, a sudden mass loss to approximately 10.6% moisture content (equivalent to 2 moles of water per 1 mol of trehalose) with no further water uptake at higher RH; the desorption isotherm shows no further water loss or gain, resulting in an open hysteresis. These events are believed to occur as a result of amorphous trehalose collapsing into its crystalline stable form, as crystalline phases are less hydrophilic than amorphous ones [34]. XRPD confirmed this assumption, since the two characteristic peaks of crystalline trehalose

Table III The Gordon-Taylor Parameter and the Fitting Coefficients by Using the Kwei Equation for the Spray Dried Composite Systems

System	Gordon-taylor equation (Eq. 7)	Kwei equation (Eq. 9)
R:HPβCD	$K_{GT} = 0.87$	$K_k = 0.25$ $q = -165.66$ $R^2 = 0.902$
T:HPβCD	$K_{GT} = 0.79$	$K_k = 1$ $q = -140.15$ $R^2 = 0.983$

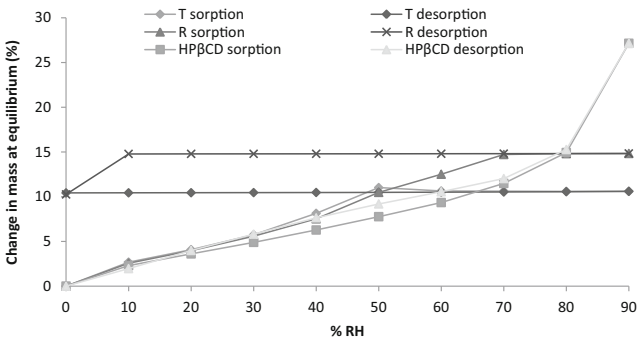

Fig. 9 Water vapour sorption and desorption isotherms of raffinose (R), trehalose (T) and hydroxypropyl-β-cylcodextrin (HPβCD) spray dried alone.

dihydrate (at 8.7 and 23.8°) were identified in the sample after DVS analysis (the XRPD are provided in the supplementary material associated with this article as Fig. 1Sa) [49–51]. Hancock and Shamblin [11] described how the maximum amount of water absorbed by amorphous sugars is usually limited by crystallisation of the sugar at high relative humidities. Therefore the critical RH for trehalose NPMPs (above which point crystallization occurrs) was identified as 50% RH.

Amorphous raffinose, also a highly hygroscopic sugar, was able to sorb approximately 14% of its weight in moisture below 70% RH (4 mol of water per 1 mol of raffinose), after which no further water uptake was registered (Fig. 9). The final water uptake after the desorption profile was 10% (*w*/*w*) (3 mol of water per 1 mol of raffinose) and an open hysteresis

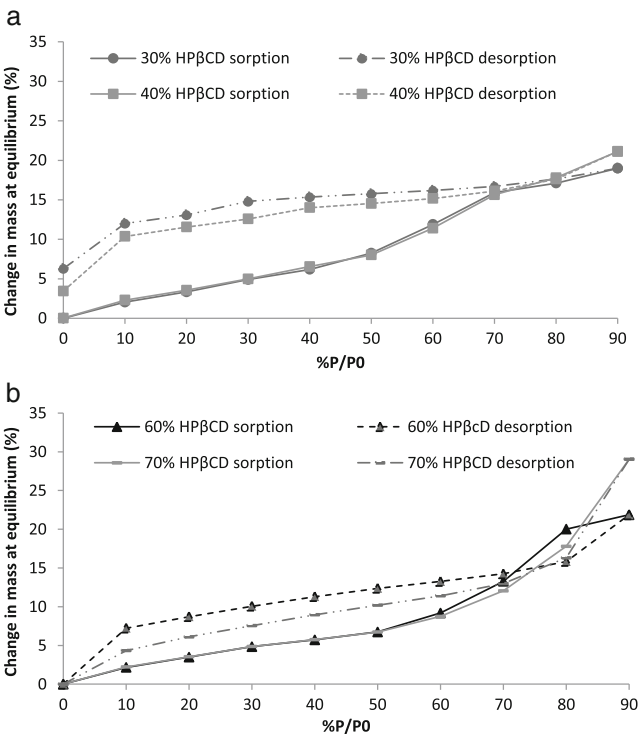

Fig. 10 Water vapour sorption and desorption isotherms (**a** and **b**) of R:HPβCD composite systems.

was recorded. XRPD showed there was recrystallisation to some extent, since the characteristic peaks of raffinose pentahydrate were present (10.75, 13.65 and 21.1°), but with very small intensity compared to the pentahydrate crystalline counterpart (the XRPD are provided in the supplementary material associated with this article as Fig. 1Sb); formation of raffinose trihydrate was hypothesised, but never confirmed. Studies by Cheng and Lin [41] have attempted to explain the hydration of raffinose when exposed to high relative humidities suggesting the formation a hydrate form that was different to the pentahydrate. Likewise, Hogan and Buckton [14] and Chamarthy *et al.* [15] have shown that raffinose was able to absorb 4 mol of water per 1 mol of raffinose when exposed to 75% RH, collapsing into its crystalline pentahydrate form. The critical RH for raffinose NPMPs was determined to be 70% RH.

Hydroxypropyl-β-cyclodextrin presented a high capacity for moisture uptake; approximately 27% change in mass was observed at the end of the sorption cycle (13.6 mol of water to 1 mol of HPβCD), that is, at 90% RH. On desorption only a small hysteresis loop was observed, and all moisture was released. Hence, the sorption/desorption isotherm presented the characteristic type IV shape according to Gregg and Sing [52] and Sing [53]. The hysteresis can be due to bulk absorption, since we have an amorphous material [11]. On the other hand, since our powder was constituted by porous particles with high surface area (Fig. 3) and presented an isotherm type IV, it is assumed that capillary condensation could also be the cause of the observed hysteresis [52]. The XRPD showed the cyclodextrin to be amorphous after DVS analysis, presenting a diffractogram similar to the unprocessed material (the XRPD are provided in the supplementary material associated with this article as Fig. 1Sc).

The water vapour sorption and desorption isotherms for R:HPβCD spray dried composite systems are presented in Fig. 10a and b. The sorption isotherms of the systems containing HPβCD in a weight fraction of 30 and 40% showed an inflection point at 70% RH, after which water uptake continued, resulting in an increase of 5 to 7% of total water sorption by these composite systems when compared to raffinose alone (which registered ~14% water sorption). The respective desorption isotherms showed an initial mass loss at higher RH followed by a constant mass loss until 10% RH after which there is a greater rate of mass loss, resulting in an open hysteresis. Final moisture uptake was ~6 and ~3%. The inflection point at 70% RH was presumed to be due to raffinose recrystallisation for the system comprising 30% weight fraction of HPβCD, as confirmed by XRPD analysis (the XRPD are provided in the supplementary material associated with this article as Fig. 2Sb). The remaining water sorption and desorption was due to the cyclodextrin-water interactions. XRPD analysis for the system with 40% weight fraction of HPβCD showed an amorphous halo with no trace of peaks, thus it was not possible to confirm raffinose recrystallisation (the XRPD are provided in the supplementary material associated with this article as Fig. 2Sc).

Spray drying of raffinose with HPβCD at a weight fraction ≥60% produced powders with a high capacity for moisture uptake; a maximum of 30% mass gain could be achieved, similar to the moisture uptake of HPβCD when spray dried alone. The sorption isotherm of powder with 60% HPβCD presented an inflection point at 80% RH with no mass loss and continuous water uptake. Desorption isotherms showed complete water desorption. Two hysteresis loops were seen: a loop between 70 and 90% RH and a second between 0 and 70% RH. XRPD revealed systems were still amorphous post DVS analysis (the XRPD are provided in the supplementary material associated with this article as Fig. 2Sd and e).

Sorption and desorption isotherms for T:HPβCD are represented in Fig. 11a and b. As different weight fractions of HPβCD (20, 30 and 40%) were spray dried with trehalose an increase in the critical relative humidity to 60% RH was observed, with a water uptake of ~12% (systems T:HPβCD 80:20, 70:30 and 60:40). Above 60% RH there was a small mass loss of ~2% followed by water uptake. Desorption isotherms showed an initial mass loss at higher RH; a constant mass from 60 to 40% and a continuous mass loss from 40 to 0% RH. Final moisture uptake was ~5%. The inflection point at 60% RH was due to trehalose recrystallisation, as was evident by XRPD analysis (the XRPD are provided in the supplementary material associated with this article as

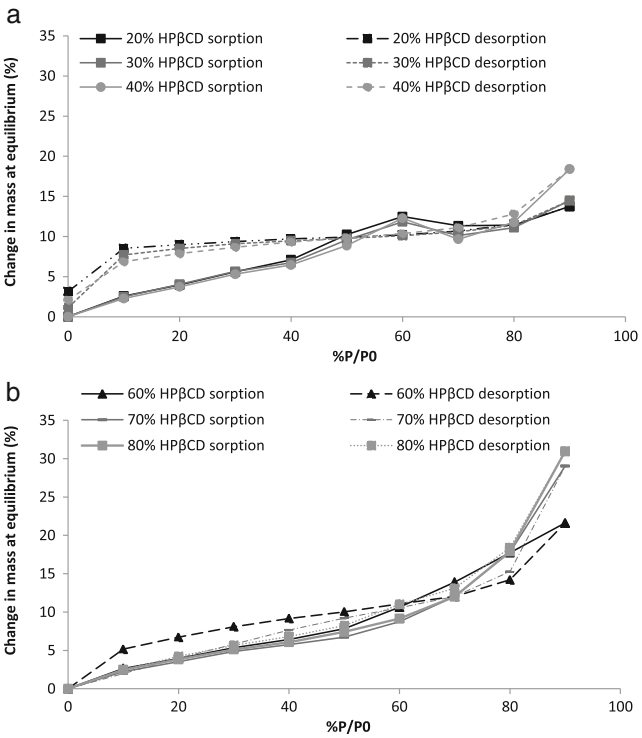

Fig. 11 Water vapour sorption and desorption isotherms of T:HPβCD composite systems.

Table IV Correlation Coefficients (R^2) and Parameters Values Estimated from Young–Nelson Model for the Different R:HPβCD Composite Systems. A = Adsorption B = Absorption

	0%	30%	40%	60%	70%	100%
A × 100	1.0	1.6	2.1	2.7	3.5	4.3
B × 100	15.0	14.3	13.6	10.5	6.6	0.065
R^2	0.958	0.991	0.990	0.982	0.971	0.938

Fig. 3Sb–d). The remaining water sorption and desorption was due to the cyclodextrin-water interactions.

When trehalose was spray dried with HPβCD weight fractions ≥60%, moisture uptake was greatly enhanced. A maximum of 30% mass gain could be achieved, similar to moisture uptake by HPβCD when spray dried alone and to R:HPβCD composite systems. The sorption/desorption isotherms could be described as type IV. Different hysteresis loops were seen: 60 and 70% HPβCD composites presented a loop between 70 and 90% RH and a second one between 0/10 and 70% RH. XRPD after DVS revealed systems were still amorphous and that a possible recrystallisation of trehalose was not evident (the XRPD are provided in the supplementary material associated with this article as Fig. 3Se–g).

The Young-Nelson model was fitted to the DVS data in order to better comprehend the water vapour isotherms. This model divides moisture sorption into three basic mechanisms: surface adsorption, multilayer adsorption (or any kind of condensation effect in general) and bulk absorption [33, 34, 54] (the Young-Nelson components plot for the materials spray dried alone are provided in the supplementary material associated with this article as Fig. 4S). Tables IV and V present the correlation coefficient (R^2) and parameters estimated (A = adsorption, B = absorption) from the Young–Nelson model for the different composite systems. The model presented good fitting for all composite systems. HPβCD presented almost no absorption, having a very low B value, adsorbing water at its surface forming a multilayer above 10% RH (Fig. 4Sc in supplementary material associated with this article). In contrast both raffinose and trehalose presented bulk absorption of water, as can be seen on Fig. 4Sa and b (in supplementary material associated with this article) and by the high value of parameter B (Tables IV and V). The composite systems showed an increase in powder capacity to adsorb water as the fraction of cyclodextrin was increased, as the A parameter increased with higher fractions of HPβCD (Tables IV and V) and the B parameter (absorption) reduced in its value. The increase in adsorption capacity of the composite systems containing cyclodextrin was expected, as this material presented no water absorption (Fig. 4Sc in supplementary material associated with this article).

In vitro deposition analysis was performed on samples presenting high SSA (≥90 m^2/g) and improved physical stability; thus selected samples were: R:HPβCD 60:40, 40:60 and 30:70; T:HPβCD 70:30, 60:40, 40:60 and 30:70.

Deposition profiles of R:HPβCD and T:HPβCD composite systems are represented in Figs. 12 and 13. The addition of cyclodextrin resulted in an evident improvement of the aerosol deposition when compared to powders comprised of raffinose or trehalose alone, with less deposition in the mouthpiece adaptor and induction port, higher deposition on stages with lower cut-off points (≤2 μm, stages 4 to 7), and increase in the % of recovered emitted dose. Fine particle fractions <3 μm and <5 μm for the R:HPβCD systems were approximately 2 fold higher ($p = 0.001$) than for raffinose spray dried alone, and the fine particle fractions <3 μm and 5 μm for T:HPβCD composite systems were approximately 4 fold higher ($p < 0.05$) than for trehalose spray dried alone (Tables VI and VII). The mass median aerodynamic diameters (MMAD) of R:HPβCD and T:HPβCD were half of the MMAD, and significantly different ($p < 0.05$), to those of raffinose and trehalose spray dried alone (Tables VI and VII).

DISCUSSION

Composite NPMPs were produced by spray drying mixtures of carbohydrates. The formation of nanoporous/nanoparticulate microparticles (NPMPs) has been reported by Healy *et al.* [31], Ní Ógaín *et al.* [6] and Paluch *et al.* [55], where the particle formation has been shown to be dependent on the solvent/anti-solvent ratio and the material(s) solubility characteristics. These parameters (solvent ratio and solubility) will control, together with the process parameters, the production of a more or less porous particle, the porosity of which can be visualised by SEM and is consistent with increased specific surface area compared to non-porous microparticles of equivalent geometric dimensions [6, 10]. The addition of cyclodextrin to the formulation did not affect the NPMP formation, as all particles were spherical and porous. In addition, it is hypothesised that the solubility of HPβCD is higher

Table V Correlation Coefficients (R^2) and Parameters Values Estimated from Young–Nelson Model for the Different T:HPβCD Composite Systems. A = Adsorption B = Absorption

	0%	20%	30%	40%	60%	70%	80%	100%
A × 100	1.6	2.8	2.8	3.4	4.6	4.2	3.6	4.3
B × 100	8.9	6.1	5.8	5.0	3.1	1.5	0.8	0.065
R^2	0.912	0.978	0.988	0.984	0.984	0.963	0.974	0.938

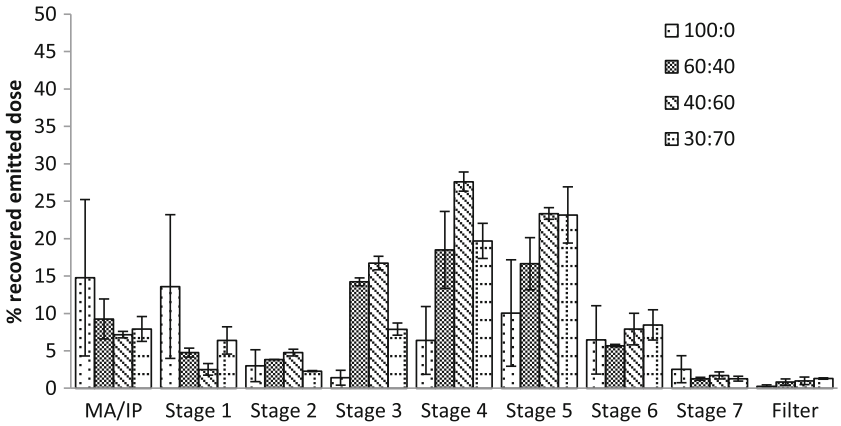

Fig. 12 *In vitro* aerosol deposition profile by use of a NGI of R:HPβCD composite systems at ratios 100:0, 60:40, 40:60 and 30:70 as calculated % of recovered emitted dose *vs.* NGI stages. MA – mouth adapter IP – induction port.

than raffinose or trehalose in the solvent system used, which, on spray drying, leads to the formation of more nanoparticulates within the microparticle as the anti-solvent evaporates, hence leading to particles with high porosity and high surface area. However, it must be born in mind that there is no linear relationship between cyclodextrin concentration and SSA/porosity (Tables I and II). In general, the composite systems presented higher SSA than raffinose or trehalose spray-dried alone.

FTIR spectra of all spray dried composite systems showed interactions between molecules. All molecules (HPβCD, raffinose and trehalose) are good H-bond donors and acceptors (hydroxyl groups). Modifications in the O-H bands are thus anticipated and may be attributed to the formation of H-bonds between raffinose or trehalose and HPβCD. The hydrogen bonds between the non-reducing sugars and the cyclodextrin are expected to be established on the external surface of the latter, which is polar (hydrophilic) due to the presence of secondary and primary hydroxyls at the edge of the ring. The inner part of the cyclodextrin is made apolar (hydrophobic) by glycosidic oxygen and methane protons [26]. Hence, it will not establish H-bonds with the sugars. Furthermore, inclusion complexes should not be formed, since the sugars are not hydrophobic and present a molecular diameter larger than the cyclodextrin cavity diameter (11.4 Å for raffinose, 12.2 Å for trehalose and 7.8 Å for the HPβCD cavity) [56–58].

Interactions between the components of the composites were also identified by the thermal behaviour, that is, by the existence of a single T_g higher than that of the single non-reducing sugar systems. Also, such interactions resulted in the inhibition of trehalose crystallisation on heating in the DSC. These composite systems were thus more thermo-physically stable when subjected to increasing temperature on the DSC than raffinose and trehalose spray dried alone.

The Gordon Taylor equation was used to predict the T_g of the spray dried systems. However, the measured glass transitions of the spray dried composite systems did not follow the Gordon Taylor equation, presenting negative deviations. Therefore, other approaches were applied for the T_g prediction: Fox and Kwei equations, with successful data fitting using the Kwei equation. The Gordon Taylor and Fox equations do not account for interactions between the mixture components, whereas the Kwei equation is used in cases of strong interactions between components [44, 46]. According to Taylor and Zografi [59] for mixing to occur, the Gibbs free energy (ΔG_m) of mixing (difference between the enthalpy (ΔH_m) and entropy (ΔS_m) of mixing) must be negative:

$\Delta G_m = \Delta H_m - T\Delta S_m$ (Eq. 10) where T is temperature

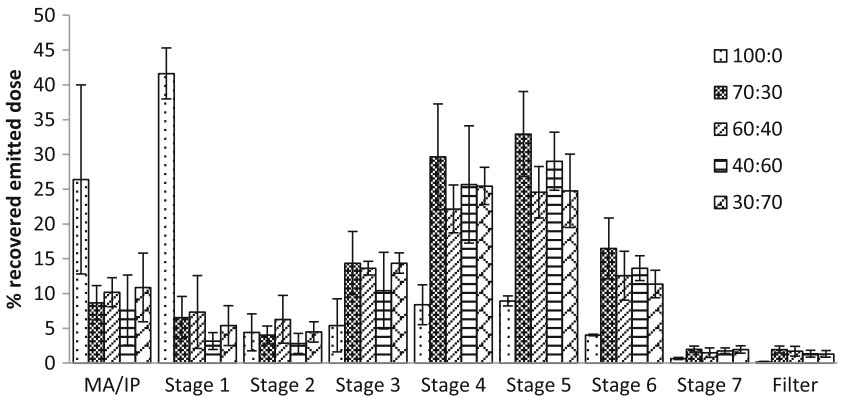

Fig. 13 *In vitro* aerosol deposition profile by use of a NGI of T:HPβCD composite systems at ratios 100:0, 70:30, 60:40, 40:60 and 30:70 as calculated % of recovered emitted dose *vs.* NGI stages. MA – mouth adapter IP – induction port.

Table VI Recovered Emitted Dose, Fine Particle Fraction (*FPF*), Mass Median Aerodynamic Diameter (*MMAD*) and Geometric Standard Deviation (*GSD*) of *in vitro* Aerosol Deposition of R:HPβCD Composite Systems. ANOVA is also Presented for Significance ($p < 0.05$) of Differences Between Means ($n = 3$, Mean ± Standard Deviation)

	R:HPβCD 0:100	R:HPβCD 60:40	R:HPβCD 40:60	R:HPβCD 30:70
% Recovered emitted dose*	68.1 ± 11.7	91.4 ± 1.2	92.7 ± 10.5	88.0 ± 1.7
FPF < 5 μm**	31.8 ± 9.9	69.5 ± 7.1	87.3 ± 0,5	81.0 ± 4.6
FPF < 3 μm**	26.4 ± 10.0	58.0 ± 8.3	83.8 ± 0.9	76.0 ± 6.1
MMAD***	4.4 ± 0.27	2.4 ± 0.07	2.2 ± 0.18	2.1 ± 0.16
GSD****	2.3 ± 0.48	2.1 ± 0.04	2.0 ± 0.04	2.1 ± 0.09

* $p = 0.020$
** $p = 0.001$
*** $p = 0.000$
**** $p = 0.689$

Three main thermodynamic effects contribute to ΔG_m: the combinatorial entropy of mixing, the free volume effect, and intermolecular interactions, by influencing the enthalpy and entropy of mixing [59].

The combinatorial entropy of mixing is always favourable when one has small molecule-small molecule and small molecule-polymer mixture, with a positive effect on entropy [59, 60]. The existence of intermolecular interactions such as hydrogen bonding will negatively contribute to ΔG_m through an increase in the entropy of the system, favouring mixing. Hence the mixtures of raffinose or trehalose with HPβCD are theoretically favourable in terms of thermodynamics.

According to Painter *et al.* [60] and Taylor and Zografi [59], this thermodynamic behaviour can be reflected in the glass transition of the system with a negative deviation from ideality (GT prediction) due to the establishment of hydrogen bonds between the different molecules, opposing H-bonding between like molecules, which would be thermodynamically closer to ideality and hence present an experimental T_g equal to the T_g predicted by the Gordon-Taylor equation. Shablim *et al.* [61] studied this effect on sucrose-PVP blends, where negative deviation to the predicted T_g were seen due to the establishment of H-bonds between the polymer and sucrose, instead of sucrose-sucrose molecules. Taylor and Zografi [59] evaluated PVP, raffinose, sucrose and trehalose blends and obtained the same results as Shablim *et al.* [61]. Therefore, based on the H-bond interactions identified by FTIR and on the *q* value of the Kwei equation, which magnitude reflects the extension of contact (H-bonds) between molecules [48]; it is thought that the detected negative deviations to the Gordon Taylor equation are due to the establishment of H-bonds between raffinose or trehalose and cyclodextrin molecules instead of H-bonds between like molecules (raffinose-raffinose or trehalose-trehalose).

DVS analysis of spray dried composite systems was used to study the effect of water vapour on the stability of the spray-dried composites, and to support the improved physical stability indicated by DSC. In both cases (R:HPβCD and T:HPβCD) a transition was seen from powder collapse into a crystalline form to maintenance of the amorphous state (inhibition of crystallisation) with increasing weight fraction of cyclodextrin, similar to the studies by Mazzobre *et al.* [22], where trehalose crystallization was delayed and inhibited by the addition of maltodextrin.

The isotherms of the spray-dried composite systems showed an increase in water sorption with increasing weight fraction of cyclodextrin. Young-Nelson model fitting demonstrated that the water vapour molecules were preferentially adsorbed (high parameter A) rather than absorbed (low parameter B). HPβCD has an amorphous nature, with high capacity for water adsorption as seen in Fig. 4Sc and by the value of Young-Nelson parameter A (Tables IV and V). Water adsorption and subsequent monolayer formation is ruled by the water affinity to the molecular groups presented by the material; HPβCD presents a highly hydrophilic external surface (OH groups) to which the water molecules bond and a hydrophobic internal surface that repels water, leading to the absence of absorption. Thus, when the cyclodextrin is combined with raffinose or trehalose, the systems gain more hydrophilic groups increasing the monolayer capacity and hydrophobic regions preventing water absorption and reducing water availability for bulk absorption by raffinose or trehalose molecules, and consequent recrystallisation.

The hysteresis events seen are attributed to the porous nature of the particles. Capillary condensation is a common phenomenon occurring in porous material; the adsorbed water from the multilayers condenses upon filling of the pore [52]. The velocity (diffusion) of water removal (desorption) is usually slower than the adsorption, leading to a difference

Table VII Recovered Emitted Dose, Fine Particle Fraction (*FPF*), Mass Median Aerodynamic Diameter (*MMAD*) and Geometric Standard Deviation (*GSD*) of *in vitro* Aerosol Deposition of T:HPβCD Composite Systems. ANOVA is also Presented for Significance ($p < 0.05$) of Differences Between Means ($n = 3$, Mean ± Standard Deviation)

	T:HPβCD 0:100	T:HPβCD 70:30	T:HPβCD 60:40	T:HPβCD 40:60	T:HPβCD 30:70
% Recovered emitted dose**	81.0 ± 12.1	90.1 ± 0.6	90.9 ± 0.7	88.9 ± 2.9	91.1 ± 1.6
FPF < 5 μm*	27.4 ± 7.6	84.2 ± 3.4	80.3 ± 6.5	83.8 ± 6.3	86.2 ± 2.7
FPF < 3 μm*	21.4 ± 2.1	81.8 ± 1.5	74.6 ± 9.9	79.9 ± 8.1	83.0 ± 3.4
MMAD*	4.4 ± 0.35	2.0 ± 0.68	2.3 ± 0.52	2.0 ± 0.24	2.2 ± 0.29
GSD***	2.6 ± 0.02	2.0 ± 0.34	2.1 ± 0.11	2.0 ± 0.11	2.0 ± 0.07

* $p = 0.000$

** $p = 0.001$

*** $p = 0.033$

between the sorption and desorption isotherms that constitutes the hysteresis. The other factor leading to hysteresis is water absorption to the powder bulk, which was confirmed by the Young-Nelson parameter B, which was higher for powders with large fractions of raffinose or trehalose.

The spray-dried composite systems were developed with a potential application in pulmonary delivery, however it is known that the main difficulty associated with aerosolization of drug powders and their efficient delivery is the strong interparticle forces which make the cohesive bulk powder agglomerate; these interparticulate forces are generally affected by surface roughness, geometrical structure and deformation of individual particles [62]. Studies by Vanbever *et al.* [63], Healy *et al.* [31], Nolan *et al.* [64] and Ní Ógáin *et al.* [6] have reported on the suitability of porous particles for pulmonary delivery of drugs. The powders presented in this study also presented suitable deposition profiles and aerodynamic characteristics, with additional improvement upon cyclodextrin inclusion in the formulation (Figs. 12 and 13, Tables VI and VII). A possible explanation for the better deposition is the enhancement of particle morphology and physicochemical characteristics. Amaro *et al.* [10] have concluded that for NPMP powders of similar particle size but differing SSA, a trend of increasing FPF with increasing SSA, attributable to the porosity of the particles is evident. This relationship between SSA and FPF was also observed for the spray dried composite systems in the current study, where R:HPβCD and T:HPβCD composite systems with similar particle size to that of raffinose or trehalose NPMPs and a SSA approximately 2-fold higher presented better *in vitro* deposition. In addition the MMADs determined for systems containing HPβCD were smaller and closer to the geometric median particle size than those of raffinose or trehalose NPMPs. One possible explanation for the lower MMADs relates to the particle morphology and respective SSA (reflecting porosity); the higher porosity of the microparticle the fewer the contact areas between particles, resulting in weaker/less cohesive aggregates and easier powder dispersion, as postulated by Tabor [65].

CONCLUSION

Nanoporous/nanoparticulate microparticles of composite systems of raffinose:HPβCD and trehalose:HPβCD can be produced by spray-drying; particles were spherical and porous as previously reported in studies by Ní Ógáin *et al.* [6] and Amaro *et al.* [10], constituting novel NPMPs powders for oral inhalation.

Particles presented suitable and enhanced (in comparison with raffinose and trehalose spray-dried alone) characteristics for pulmonary delivery, with recovered emitted doses of approximately 90%, fine particle fraction as per emitted dose <5 μm between 70 and 90% and a median mass aerodynamic diameter of approximately 2 μm.

HPβCD acted as a thermal stability enhancer by increasing the glass transition temperature of the spray dried systems. The glass transition behavior of the spray dried blends deviates from the commonly used predictions by the Gordon-Taylor equation. These deviations were attributed to the establishment of hydrogen bonds between the cyclodextrin and non-reducing sugar molecules.

The Young-Nelson model was successfully fitted to the sorption data, allowing further explanation of the crystallization delay and inhibition of raffinose and trehalose by the presence of HPβCD, with reduction of absorption and increase in the adsorption with higher concentrations of cyclodextrin proving the increased water scavenger capacity of the system by the inclusion of HPβCD

To conclude, the co-spray drying of raffinose or trehalose with hydroxypropyl-β-cyclodextrin results in powders with improved physicochemical characteristics, physical stability

and aerosolization, suggesting their potential as carrier systems for biomolecules for pulmonary delivery.

ACKNOWLEDGMENTS AND DISCLOSURES

This publication has emanated from research conducted with the financial support of Science Foundation Ireland (SFI) under Grant Number 07/SRC/B1154 and Grant Number SFI/12/RC/2275.

REFERENCES

1. Colaço C, Sen S, Thangavelu M, Pinder S, Roser B. Extraordinary Stability of Enzymes Dried in Trehalose: Simplified Molecular Biology. Bio/Technology. 1992;10:1007–11. 1.
2. Johnson K. Preparation of peptide and protein powders for inhalation. Adv. Drug Deliv. Rev. Elsevier Sci B.V.; 1997;26:3–15.
3. Maury M, Murphy K, Kumar S, Shi L, Lee G. Effects of process variables on the powder yield of spray-dried trehalose on a laboratory spray-dryer. Eur J Pharm Biopharm. 2005;59:565–73.
4. López-Díez EC, Bone S. The interaction of trypsin with trehalose: an investigation of protein preservation mechanisms. Biochim Biophys Acta. 2004;1673:139–48.
5. Yoshii H, Buche F, Takeuchi N, Terrol C, Ohgawara M, Furuta T. Effects of protein on retention of ADH enzyme activity encapsulated in trehalose matrices by spray drying. J Food Eng. 2008;87:34–9.
6. Ogáin ON, Li J, Tajber L, Corrigan OI, Healy AM. Particle engineering of materials for oral inhalation by dry powder inhalers. I-Particles of sugar excipients (trehalose and raffinose) for protein delivery. Int J Pharm. 2011;405:23–35.
7. Carpenter JF, Crowe JH. The mechanism of cryoprotection of proteins by solutes. Cryobiology. 1988;25:244–55.
8. Carpenter JF, Crowe JH. An infrared spectroscopic study of the interactions of carbohydrates with dried proteins. Biochemistry. 1989;28:3916–22.
9. Franks F, Hatley RHM, Mathias SF. Materials science and the production of shelf-stable biologicals. Biopharm-the Technol Bus Biopharm. 1991;4:38–41.
10. Amaro M, Tajber L, Corrigan O, Healy A. Optimisation of spray drying process conditions for sugar nanoporous microparticles (NPMPs) intended for inhalation. Int J Pharm. 2011;421:99–109.
11. Hancock BC, Shamblin SL. Water vapour sorption by pharmaceutical sugars. Pharm Sci Technol Today. 1998;1:345–51.
12. Yu L. Amorphous pharmaceutical solids: preparation, characterization and stabilization. Adv Drug Deliv Rev. 2001;48:27–42.
13. Newman A, Knipp G, Zografi G. Assessing the performance of amorphous solid dispersions. J. Pharm. 2012;1–23.
14. Hogan SE, Buckton G. Water sorption/desorption–near IR and calorimetric study of crystalline and amorphous raffinose. Int J Pharm. 2001;227:57–69.
15. Chamarthy SP, Khalef N, Trasi N, Bakri A, Carvajal MT, Pinal R. The effect of dehydration conditions on the functionality of anhydrous amorphous raffinose. Eur J Pharm Sci. 2010;40:171–8.
16. Schebor C, Mazzobre MF, Buera MDP. Glass transition and time-dependent crystallization behavior of dehydration bioprotectant sugars. Carbohydr Res. 2010;345:303–8.
17. Sun W, Davidson P. Protein inactivation in amorphous sucrose and trehalose matrices: effects of phase separation and crystallization. Biochim Biophys Acta. 1998;1425:235–44.
18. Davidson P, Sun WQ. Effect of sucrose/raffinose mass ratios on the stability of co-lyophilized protein during storage above the Tg. Pharm Res. 2001;18:474–9.
19. Buera P, Schebor C, Elizalde B. Effects of carbohydrate crystallization on stability of dehydrated foods and ingredient formulations. J Food Eng. 2005;67:157–65.
20. Leinen KM, Labuza TP. Crystallization inhibition of an amorphous sucrose system using raffinose. J Zhejiang Univ Sci B. 2006;7:85–9.
21. Sinha S, Baboota S, Ali M, Kumar A, Ali J. Solid dispersion: an alternative technique for bioavailability enhancement of poorly soluble drugs. J Dispers Sci Technol. 2009;30:1458–73.
22. Mazzobre MF, del Pilar BM, Chirife J. Protective role of trehalose on thermal stability of lactase in relation to its glass and crystal forming properties and effect of delaying crystallization. LWT-Food Sci Technol. 1997;30:324–9.
23. Loftsson T, Brewster ME. Pharmaceutical applications of cyclodextrins. 1. Drug solubilization and stabilization. J Pharm Sci. 1996;85:1017–25.
24. Muñoz-Ruiz A. Particle and powder properties of cyclodextrins. Int J Pharm. 1997;148:33–9.
25. Davis ME, Brewster ME. Cyclodextrin-based pharmaceutics: past, present and future. Nat Rev Drug Discov. 2004;3:1023–35.
26. Shao Z, Krishnamoorthy R, Mitra AK. Cyclodextrins as nasal absorption promoters of insulin: mechanistic evaluations. Pharm Res. 1992;9:1157–63.
27. Branchu S, Forbes RT, York P, Petrén S, Nyqvist H, Camber O. Hydroxypropyl-beta-cyclodextrin inhibits spray-drying-induced inactivation of beta-galactosidase. J Pharm Sci. 1999;88:905–11.
28. Bosquillon C, Lombry C, Préat V, Vanbever R. Influence of formulation excipients and physical characteristics of inhalation dry powders on their aerosolization performance. J Control Release. 2001;70:329–39.
29. Bosquillon C, Lombry C, Preat V, Vanbever R. Comparison of particle sizing techniques in the case of inhalation dry powders. J Pharm Sci. 2001;90:2032–41.
30. Maa YF, Costantino HR, Nguyen PA, Hsu CC. The effect of operating and formulation variables on the morphology of spray-dried protein particles. Pharm Dev Technol. 1997;2:213–23.
31. Healy AM, McDonald BF, Tajber L, Corrigan OI. Characterisation of excipient-free nanoporous microparticles (NPMPs) of bendroflumethiazide. Eur J Pharm Biopharm. 2008;69:1182–6.
32. Burnett D, Thielmann F. Impact of Protein Concentration on the Moisture-Induced Phase Transitions of Protein-Sugar Formulations. Amer. Biotech, Lab. 2006;1–10.
33. Bravo-Osuna I, Ferrero C, Jiménez-Castellanos MR. Water sorption–desorption behaviour of methyl methacrylate-starch copolymers: effect of hydrophobic graft and drying method. Eur J Pharm Biopharm. 2005;59:537–48.
34. Tewes F, Tajber L, Corrigan OI, Ehrhardt C, Healy AM. Development and characterisation of soluble polymeric particles for pulmonary peptide delivery. Eur J Pharm Sci. 2010;41:337–52.
35. European pharmacopoeia. Preparations for inhalation: Aerodynamic assessment of fine particles. 7th Editio. Strasbourg; 2012. p. 274–84.
36. Murthy NS, Minor H, Bednarczyk C, Krimm S. Structure of the amorphous phase in oriented polymers. Macromolecules. 1993;25:1712–21.
37. Bosquillon C, Rouxhet PG, Ahimou F, Simon D, Culot C, Préat V, *et al.* Aerosolization properties, surface composition and physical state of spray-dried protein powders. J Control Release. 2004;99:357–67.
38. Wolkers WF, Oldenhof H, Alberda M, Hoekstra FA. A fourier transform infrared microspectroscopy study of sugar glasses: application to anhydrobiotic higher plant cells. Biochim Biophys Acta. 1998;1379:83–96.
39. Akao K, Okubo Y, Asakawa N, Inoue Y, Sakurai M. Infrared spectroscopic study on the properties of the anhydrous form II of

trehalose. Implications for the functional mechanism of trehalose as a biostabilizer. Carbohydr Res. 2001;334:233–41.
40. Wolkers WF, Oliver AE, Tablin F, Crowe JH. A fourier-transform infrared spectroscopy study of sugar glasses. Carbohydr Res. 2004;339:1077–85.
41. Cheng W-T, Lin S-Y. Processes of dehydration and rehydration of raffinose pentahydrate investigated by thermal analysis and FT-IR/DSC microscopic system. Carbohydr Polym. 2006;64:212–7.
42. Misiuk W, Zalewska M. Investigation of inclusion complex of trazodone hydrochloride with hydroxypropyl-β-cyclodextrin. Carbohydr Polym. 2009;77:482–8.
43. Wu X, Li X, Mansour H. Surface analytical techniques in solid-state particle characterization for predicting performance in dry powder inhalers. KONA Powder Part J. 2010;28:3–19.
44. Yavuz B, Bilensoy E, Vural I, Sumnu M. Alternative oral exemestane formulation: improved dissolution and permeation. Int J Pharm. 2010;398:137–45.
45. Kalichevsky MT, Jaroszkiewicz EM, Blanshard JMV. A study of the glass transition of amylopectin—sugar mixtures. Polymer. 1993;34:346–58.
46. Chen T, Bhowmick S, Sputtek A, Fowler A, Toner M. The glass transition temperature of mixtures of trehalose and hydroxyethyl starch. Cryobiology. 2002;44:301–6.
47. Tajber L, Corrigan OI, Healy AM. Physicochemical evaluation of PVP-thiazide diuretic interactions in co-spray-dried composites–analysis of glass transition composition relationships. Eur J Pharm Sci. 2005;24:553–63.
48. Kwei TK. The effect of hydrogen bonding on the glass transition temperatures of polymer mixtures. J Polym Sci Polym Lett Ed. 1984;22:307–13.
49. Nagase H, Endo T, Ueda H, Nakagaki M. An anhydrous polymorphic form of trehalose. Carbohydr Res. 2002;337:167–73.
50. Pinto SS, Moura-ramos JJ. Crystalline anhydrous-trehalose (polymorph b) and crystalline dihydrate a, a -trehalose : A calorimetric study. J Chem Thermodyn. 2006;38:1130–8.
51. Ohashi T, Yoshii H, Furuta T. Innovative crystal transformation of dihydrate trehalose to anhydrous trehalose using ethanol. Carbohydr Res. 2007;342:819–25.
52. Gregg SJ, Sing KSW. Adsorption, surface area and porosity. 2nd ed. London: Academic; 1982.
53. Sing KSW. Reporting physisorption data for gas/solid systems with special reference to the determination of surface area and porosity (Recommendations 1984). Pure Appl. Chem. 1985;603–19.
54. Thielmann F. Hysteresis Effects in Vapour Sorption. Surf. Meas. Syst. Ltd. London: Surface Measurements Systems Ltd; 2004; 1–8.
55. Paluch KJ, Tajber L, Corrigan OI, Healy AM. Impact of process variables on the micromeritic and physicochemical properties of spray-dried porous microparticles, part I: introduction of a new morphology classification system. J Pharm Pharmacol. 2012;64:1570–82.
56. Clinkenbeard KD, Thiessen AE. Mechanism of action of Moraxella bovis hemolysin. Infect Immun. 1991;59:1148–52.
57. Brewster ME, Loftsson T. Cyclodextrins as pharmaceutical solubilizers. Adv Drug Deliv Rev. 2007;59:645–66.
58. Nagase H, Ogawa N, Endo T, Shiro M, Ueda H, Sakurai M. Crystal structure of an anhydrous form of trehalose : structure of water channels of trehalose polymorphism. J Phys Chem B. 2008;112(9):105–11.
59. Taylor LS, Zografi G. Sugar-polymer hydrogen bond interactions in lyophilized amorphous mixtures. J Pharm Sci. 1998;87:1615–21.
60. Painter PC, Graf JF, Coleman MM. Effect of hydrogen bonding on the enthalpy of mixing and the composition dependence of the glass transition temperature in polymer blends. Macromolecules. 1991;24:5630–8.
61. Shamblin SL, Taylor LS, Zografi G. Mixing behavior of colyophilized binary systems. J Pharm Sci. 1998;87:694–701.
62. Daniher DI, Zhu J. Dry powder platform for pulmonary drug delivery. Particuology. 2008;6:225–38.
63. Vanbever R, Mintzes JD, Wang J, Nice J, Chen D, Batycky R, *et al.* Formulation and physical characterization of large porous particles for inhalation. Pharm. Res. 1999;1735–42.
64. Nolan LM, Li J, Tajber L, Corrigan OI, Healy AM. Particle engineering of materials for oral inhalation by dry powder inhalers. II-Sodium cromoglicate. Int J Pharm. 2011;405:36–46.
65. Tabor D. Surface forces and surface interactions. J Colloid Interface Sci. 1977;58:2–13.